OBSERVATIONS OF MIXED-PHASE CLOUDS USING AIRBORNE LIDAR AND IN-SITU INSTRUMENTATION

Iwona S. Stachlewska [1] *, Jean–Francois Gayet [2], Christophe Duroure [2], Alfons Schwarzenboeck [2], Olivier Jourdan [2], Valery Shcherbakov [3], Roland Neuber [1]

[1]Alfred-Wegener-Institute for Polar and Marine Research, Telegrafenberg A43, 14473 Potsdam, Germany
** now at Leosphere, EcolePolytechnique, 91128 Palaiseau Cedex,France, istachlewska@leosphere.fr*
[2]LaMP UMR 6016 CNRS / Université Blaise Pascal, 24 avenue des Landais, 63-177 Aubière, France
[3]Institute of Physics, Skariny av. 68, 220072 Minsk, Belarus

ABSTRACT

The airborne activities during the ASTAR 2004 [1] campaign were extended by the operation of a second AWI research aircraft Polar 2 deployed for the remote measurements of vertical distribution of aerosol and thin cloud optical properties with the AWI Airborne Mobile Aerosol Lidar (AMALi) [2], as well as for the in-situ measurements of the microphysical and optical properties of Arctic clouds (particularly ice phase in mixed-phase clouds) by an unique combination of LaMP instrumentation. It allowed development of an experimental methodology for the description of the cloud properties using alternated remote and in-situ observations. In this paper the results obtained during the flight on 5 June 2004, taken under the requirement that both lidar and in-situ instrumentation probe the same cloud system are presented. Quasi-simultaneous alternated remote observations of clouds vertical and horizontal structures and depolarisation effects due to presence of ice particles are combined with in-situ microphysics and optical properties of cloud particles.

1. INTRODUCTION

The investigations of climate change due to changes of the cloud radiative properties (altitude, area coverage and cloud properties), the indirect effect of aerosols on cloud formation, and the cloud modification on ice pack, are important in climatologically pivotal areas such as the Arctic. The information on the properties of arctic clouds is scant, which makes the modelling of aerosol-cloud-climate interactions challenging.
The measurements carried out during ASTAR 2004 campaign in the vicinity of Svalbard Archipelago well contribute to such collaborative studies. Svalbard is a well-fitting spot to assess these scientific issues by utilising its permanently maintained research stations (Koldewey, Rabben, Zeppelin, Hornsund), access to logistics for research aircrafts (Longyearbyen and Ny Ålesund airports), space observations (MODIS, and in future CALIPSO, CLOUDSAT). Additionally, the Svalbard's atmosphere characterised by 'laboratory-like' transitions from 'polluted-to-clean' conditions in Springtime which makes the analysis and interpretation of the measurements easier as in the mid-latitudes.

2. METHODOLOGY

In this paper the observations of a partly glaciated stratocumulus cloud deck over Storfjorden between 7:40-11:35 UT on 5 June 2004 are analysed.
During this flight (Fig.1) firstly, the in-situ instruments took observations in clouds while heading North-East from Longyearbyen towards the northern part of Storfjorden. There descend and ascent in cloud was performed (8:00-8:50).
Afterwards the remote AMALi measurements were taken from a flight altitude of approximately 3km, while heading strait into southern part of Storfjorden (9:00-10:20). During these observations the cloud structures were observed over an ice covered northern part of the fiord and the background aerosol profiles were taken in a cloud-free area over open water just outside the fiord.

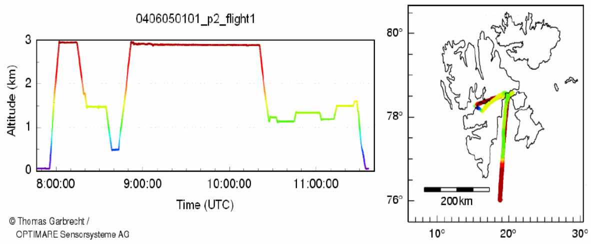

Fig.1 The flight altitude (left) and flight path (right) of the Polar2 aircraft on 5th June 2004 during the ASTAR campaign. Provided by Dr. T. Garbrecht (OPTIMARE, Germany)

Finally, after a descent into the marine stratocumulus cloud layer, the heading back along the same flight path (10:30-11:30) but at altitudes between 1.1-1.5km towards the northern end of Storfjorden while the in-situ observations were performed.
The water stratocumulus cloud top was about -12°C. At upper levels ice particles were evidenced to precipitate down to the stratocumulus layer leading to a possible feeder-seeder phenomenon within the water cloud. Therefore, three kinds of clouds with different microphysical and optical properties, i.e. precipitating ice crystals, mixed-phase cloud and water layer cloud with large drops, were evidenced from both measurements.

3. LIDAR MEASUREMENTS

The AMALi contribution to this experiment was useful in two ways. Firstly, the availability of the real-time display of the quick-look evaluation of the measured atmosphere allowed for an immediate in-flight interpretation of lidar signals at 532nm and 1064nm and a depolarisation ratio at 532nm. Hence, recognition and guidance of in-situ observations into the areas of particular research interest was possible [2]. Secondly, after the flight, the calculation of calibrated backscatter profiles at selected times along the flight path and in the regions of low density clouds was possible using the iterative airborne lidar inversion scheme [3,4].

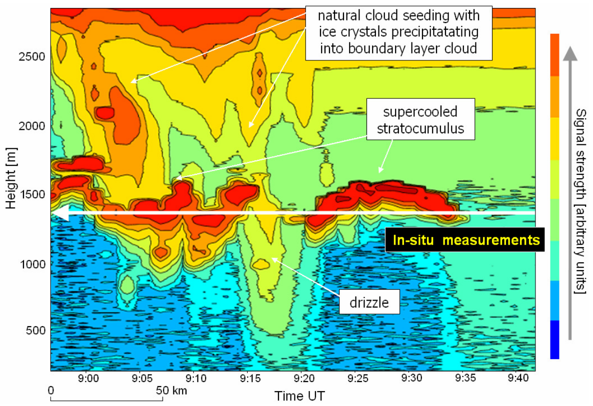

Fig.2. The vertical cross-section of the attenuated AMALi lidar signal at 532nm for measurements of the mixed-phase clouds between 8:57-9:42 on 5 June 2004 during ASTAR

The AMALi signals with corresponding depolarisation ratio at 532nm recorded during the flight sequence performed at 3km are shown in Fig.2 and Fig.3.
During the first part of the measurement, between 8:57-9:15 precipitating ice particles are clearly evidenced. At some parts of the cloud system in this time interval the ice crystals seem to reach the water cloud below (9:00-9:05 and 9:10-9:15). At the very first part of the measurements between 8:58-9:02 the double structure in a lower cloud deck with an ice cloud at an altitude of about 1.5km topped by a water cloud at about 1.75km was observed. Otherwise, the lower deck cloud contained highly concentrated spherical particles of low depolarisation ratio of 1.4-5%.
In the upper cloud layer the depolarisation ratio increases from 25-30% to 40-50% which clearly reveal the occurrence of irregularly shaped ice crystals. We may expect this ice crystals precipitation down to the water cloud layer at 1.4km altitude. Then, due to Findeisen-Bergeron process the ice crystals may grow to the detriment of supercooled water droplets as far as most of them may be consumed.
Nevertheless, the observations do not confirm this hypothesis since the precipitating down to the ground stratocumulus feature (9:16-9:21) rather highlights depolarisation ratio as low as 1.4% to 5% typical for only spherical particles and hence for freezing drizzle.

The second part of the measurements between 9:22-9:35 UT was taken in a cloud-free atmosphere above a dense liquid cloud of about 150-200m depth extending horizontally over about 65km at an altitude of about 1.5km. The laser beam in both lower deck water clouds was rapidly attenuated due to very high concentration of the scattering centres resulting in the multiple scattering. Hence, the lidar signals and depolarisation ratio below these clouds and the sea level cannot be exploited in the further analysis. The signals above these clouds reveal, due to a weaker beam attenuation, distinct cloud structures containing either large non-spherical particles or spherical particles with a lower concentration.
The final part of the measurement between 9:36-9:42 UT was taken in a cloud-free background atmosphere.
The noisy character of depolarisation ratio profiles observed in the clear atmosphere areas is due to lower target concentrations than in aerosol-rich atmosphere or in clouds resulting in a weaker backscatter signal at perpendicular 532nm wavelength. The representative mean value of depolarisation ratio of 5.4% in the clear parts of atmosphere above the water cloud and in cloud-free atmosphere between 9:25-9:42 UT was found.

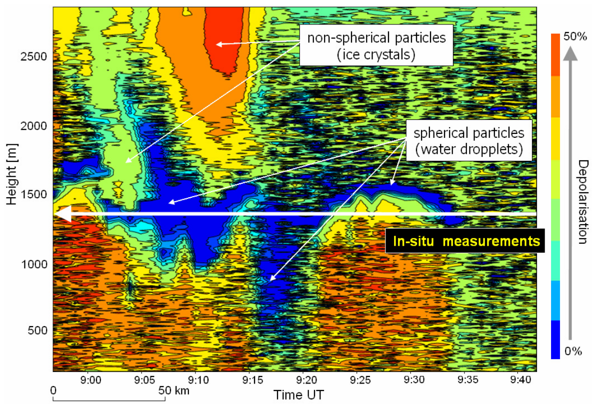

Fig.2. The vertical cross-section of the depolarisation ratio at 532nm for measurements of the mixed-phase clouds between 8:57-9:42 on 5 June 2004 during ASTAR

The calculations using the iterative airborne inversion scheme [3] allow for accurate retrieval of calibrated particle backscatter coefficient profile along the flight path using Klett's approach [5] but independently on whether and how well is known the far-field calibration value itself. A useful demonstration of a means of determining an approximate near-field boundary value and its use as a constraint for retrieval initiated in the far-field is discussed in [4]. For most retrievals of the AMALi observations under clean clear-sky conditions during ASTAR, the constant lidar ratio of 20-25sr can be assumed without hindering the solution [3,4]. For calculations in water clouds the lidar ratio can be obtained from the Mie-theory if, usually difficult, guess of the size of the particles is made. For the ice particles such calculations make hardly sense due to their non-spherical shape, however, if the clouds contain mainly ice crystals an assumption of a lidar ratio between 7-15sr is plausible. Unlike for the usual approach where the lidar ratio is estimated or simply guessed, here the iterative calculations are applied to clouds of low optical densities, which are penetrable with the laser beam without causing the multiple scattering, i.e. in the areas of the cloud system where the cloud optical depth is lower than the threshold particle optical depth of 0.065 in 100m thick layer. The accurate calculations are done with lidar ratio characteristic for type of cloud (water/ice) obtained from in-situ observations. The particle backscatter coefficient profiles obtained with such lidar ratios are presented and discussed in Sect.5.

4. IN-SITU MEASUREMENTS

The in-situ probes provided cloud characteristics in terms of particle size distribution, concentration, ice/liquid water content, morphology, scattering phase function, and refractive index and asymmetry factor.

The particle size distributions for water and ice clouds obtained form PMS 2D-C probe and the Polar Nephelometer (after inversion) is depicted on Fig.4.

Generally, in both types of clouds rather small size cloud droplets with size less than 200µm and with no super-large drops were observed. For both types of clouds the concentration of the small size particles with effective diameter around 25µm is similar but for the ice cloud a significant fraction of larger particles with effective diameter of around 200µm was measured.

The particle concentrations of $8 \cdot 10^3 l^{-1}$ with particle extinction of $10 \cdot 10^3 m^{-1}$ in water cloud and much lower concentrations of $11 l^{-1}$ and particle extinction of $0.4 \cdot 10^3 m^{-1}$ in ice cloud were retrieved. In case of a water cloud relatively high concentration of small size droplets are present with absence of large particles. On the contrary, for ice cloud, the presence of sufficiently large particles causes its 'precipitating' character.

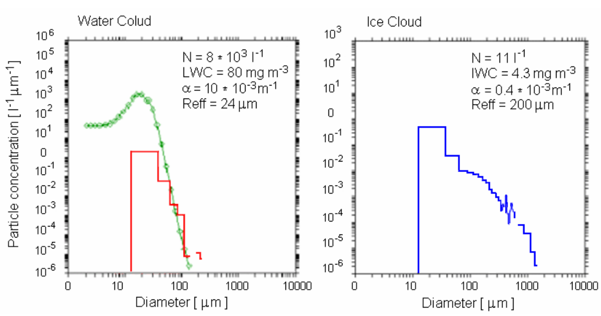

Fig.4. The particle size distributions for water cloud (left) and ice cloud (right) obtained form PMS 2D-C probe (line) and retrieved from the Polar Nephelometer measurements (dotted line) taken on 5 June 2004 during the ASTAR campaign.

The Nevzorov Probe measured $80 mgm^{-3}$ liquid water content in the water cloud and $4.3 mgm^{-3}$ ice water content in ice cloud, respectively.

The measurements of the scattering phase function for water and precipitating ice crystals obtained with the Polar Nephelometer are shown on Fig.5. Characteristic deep minimum due to the spherical particles for the the water cloud is evidenced. For each recognized cloud particle phase composition (water droplets and ice crystals) the optical parameters such as the extinction coefficient, the asymmetry factor and the lidar ratio were derived from the measured scattering phase function [6]. The lidar ratio of 14.5sr and, as expected for the ice clouds, a bit lower of 13.8sr for 532nm were obtained.

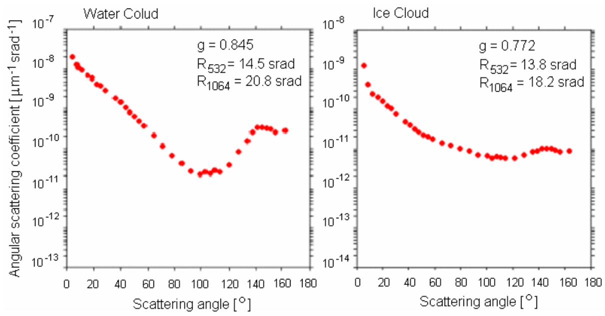

Fig.5. The scattering phase function for water cloud (left) and ice cloud (right) obtained from Polar Nephelometer for measurements on 5 June 2004 during the ASTAR campaign.

As these results (Fig.4) represent mean values obtained during sequences of 2min for the water cloud and 7min for the ice cloud, respectively, they are considered statistically reliable due to a very large sampled volume. The natural variability, generally high in any cloud types, is not considered in these results. The statistical errors on microphysical measurements are discussed in details in [7].

5. COMPARISON OF RETRIEVALS

The particle backscatter profiles obtained with 2min temporal resolution corresponding to about 8km range calculated using the iterative approach [3,4] with lidar ratios corresponding to 'ice cloud' and 'water cloud' retrieved from the in-situ measurements and 'clear air' lidar ratios assumed to be 25sr are shown in Fig.6.

The profiles no.1–3 were obtained at 9:00, 9:08 and 9:13 in the area of the precipitating ice crystals. The profile no.4 was obtained at 9:19 in the drizzle and could be retrieved down to the sea level. The profile no.5 at 9:27 was obtained in a clear atmosphere above the liquid cloud and, finally, the profile no.6 at 9:37 in the cloud-free atmosphere was calculated as a reference profile.

The lidar particle extinction coefficient of $0.07 \cdot 10^{-3} m^{-1}$ in the ice cloud area was retrieved for backscatter value of $0.5 \cdot 10^{-5} m^{-1} sr^{-1}$ estimated from particle backscatter coefficient profiles no.1-3 with corresponding 'ice cloud' lidar ratio of 13.8sr. The particle extinction coefficient of $0.61 \cdot 10^{-3} m^{-1}$ in the drizzle area was retrieved for maximum of the particle backscatter value of $4.2 \cdot 10^{-5} m^{-1} sr^{-1}$ estimated from backscatter profile no.4 with corresponding 'water cloud' lidar ratio of 14.5sr.

The in-situ particle extinction coefficient of 0.05-0.4·$10^{-3}m^{-1}$ in the ice cloud and 1-10·$10^{-3}m^{-1}$ in the drizzle was obtained.

The comparison of particle extinction from remote and direct observations shows similar values in ice clouds and significant differences in drizzle case which can be explained by the time shift between both measurements and by a possible increase of the drizzle formation.

The drizzle intensification seems also be reasonable from the analyses of the lidar signals alone. The calculations of particle backscatter profiles in 'cloudy' area is possible only within the range of mentioned threshold values of the particle extinction of less than 0.65·$10^{-3}m^{-1}$. Hence, the lidar measurements in the intense drizzle sampled by in-situ instrumentation for which the particle extinction coefficient of more than 1·$10^{-3}m^{-1}$ would not be possible, due to the multiple scattering on these drizzle particles.

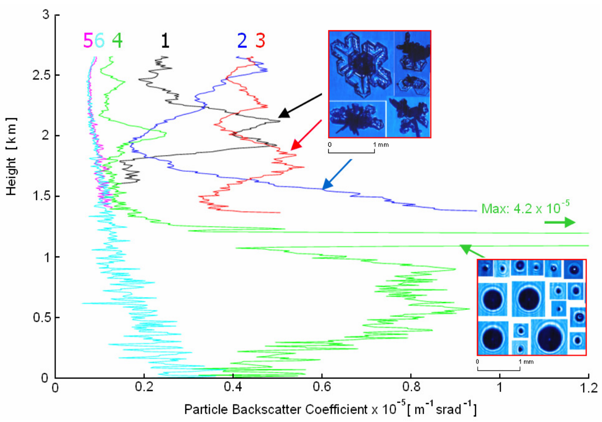

Fig.6. The particle backscatter coefficient retrieved for the pre-selected regions of the mixed-phase cloud; in ice cloud (1-3), drizzle (4), and cloud-free atmosphere (5,6) from the AMALi measurements at 532nm during the flight on 5 June 2004 at ASTAR campaign. The CPI images of the ice crystals and water droplets attribute to each type of cloud.

6. CONCLUSIONS

The airborne remote and in-situ cloud studies comprising the instrumentation onboard of the two aircrafts have been used in the 'cloud'-community before. Here are discussed first observations proving the feasibility of alternated measurement approach possible if only one aircraft is available.

The combined analysis of remote and in-situ measurements allowed for characterisation of mixed-phase Arctic clouds and for attributing different particle shapes (spherical and non-spherical) to distinct zones of the cloud system. In case of the observations of a feeder-seeder phenomenon three kinds of clouds with different microphysical and optical properties; the precipitating ice crystals, the mixed-phase cloud and the water layer cloud with large drops were found. The identification of vertical and horizontal structures of mixed-phase clouds, the identification of typical signatures of drizzle and ice clouds and the derivation of the typical 'ice-cloud' and 'liquid-cloud' lidar ratios was possible.

The cross-check of the retrieved lidar backscatter and extinction with the in-situ observations proves the feasibility of the alternated probing approach. Though, to improve the methodology more observations coordinated in space and time is necessary.

Additionally, the lidar measurements of cloud areas and their direct surrounding give an idea on the atmospheric 'dynamics', which allows constraining the open questions on whether the surrounding is entirely clear or contaminated with some cloud particles, e.g. in the case of the water drops above boundary cloud deck found in the depolarisation from 9:19 to 9:23 (Fig.3).

Finally, the approach will be continued for validation of the satellite cloud observations during future ASTAR campaigns, and the results obtained from such alternated measurements should contribute to the modelling of aerosol-cloud-climate interactions.

REFERENCES

1. Arctic Study of Thopospheric Aerosol, Clouds and Radiation, http://www.awi-potsdam.de/www-pot/astar

2. Stachlewska I.S., et al. Airborne Mobile Aerosol Lidar for measurements of arctic aerosol, *ILRC22, ESA SP-561*, 87-89, 2004

3. Stachlewska I.S., Investigation of tropospheric arctic aerosol and mixed-phase clouds using airborne lidar technique. *PhD Thesis, University of Potsdam,* urn:nbn:de:kobv:517-opus-6984, http://opus.kobv.de/ubp/volltexte/2006/698/, 2006

4. Stachlewska I.S. and Dörnbrack A., Application of iterative airborne lidar inversion and its interpretation by means of ECMWF operational analysis, *ILRC23, accepted paper*, 2006

5. Klett J.D., Lidar inversions with variable backscatter/extinction values. *Applied Optics* 24, 1638-1648, 1985

6. Jourdan O., et al. Assessment of cloud optical parameters in the solar region: Retrievals from airborne measurements of scattering phase functions, *Journal of Geophysical Research,* Vol.108, 4572, doi:10.1029/2003JD003493 (AGU), 2003

7. Gayet J.-F., et al. Two case studies of winter continental-type water and mixed-phase stratocumuli over the sea 1. Microphysical and optical properties, *Journal of Geophysical Research,*J., 107, No. D21, 4569, DOI 10.1029/2001JD001106 (AGU), 2002